Computational study of the vortex path variation with the VG height

2014 J. Phys.: Conf. Ser. 524 012024

(http://iopscience.iop.org/1742-6596/524/1/012024)

Computational study of the vortex path variation with the VG height

U. Fernández-Gámiz[1], G. Zamorano[1] and E. Zulueta[2]

[1]Nuclear Engineering and Fluid Mechanics Dep., University of the Basque Country, Nieves Cano 12, 01006 Vitoria-Gasteiz, Araba, Spain

[2]Automatic and Simulation Dep., University of the Basque Country, Nieves Cano 12, 01006 Vitoria-Gasteiz, Araba, Spain

E-mail: `unai.fernandez@ehu.es`

Abstract. An extensive range of conventional, vane-type, passive vortex generators (VGs) are in use for successful applications of flow separation control. In most cases, the VG height is designed with the same thickness as the local boundary layer at the VG position. However, in some applications, these conventional VGs may produce excess residual drag. The so-called low-profile VGs can reduce the parasitic drag associated to this kind of passive control devices. As suggested by many authors, low-profile VGs can provide enough momentum transfer over a region several times their own height for effective flow-separation control with much lower drag. The main objective of this work is to study the variation of the path and the development of the primary vortex generated by a rectangular VG mounted on a flat plate with five different device heights $h = \delta$, $h_1 = 0.8\delta$, $h_2 = 0.6\delta$, $h_3 = 0.4\delta$ and $h_4 = 0.2\delta$, where δ is the local boundary layer thickness. For this purpose, computational simulations have been carried out at Reynolds number $Re = 1350$ based on the height of the conventional VG $h = 0.25m$ with the angle of attack of the vane to the oncoming flow $\beta = 18.5°$. The results show that the VG scaling significantly affects the vortex trajectory and the peak vorticity generated by the primary vortex.

1. Introduction

Due to large energy losses associated with boundary-layer separation, flow separation control has become a very important issue for several industrial applications in the field of fluid mechanics. The most important reason of flow-separation is the lack of momentum in the boundary layer, thus usually the primary option in trying to control the flow separation is the installation of vortex generators because they have the advantage of being cost-effective and simple to set-up and manufacture. Flow control devices can be used to increase both free-shear and wall-bounded flows by extending the effective area through which transport occurs, by setting off resonant flow instabilities, by advancing laminar to turbulent transition and by enhancing the turbulence once the shear flow is already turbulent, Gad-el-Hak [1]. The effective generation of secondary flows and/or recirculation areas is an additional tool with which to enhance mixing in both laminar and turbulent flows. The use of vortex generators is a successful example of this strategy.

Many models for the generated vortices have been presented over the years. Theoretical models include, for example, the one by Smith [2] and a model presented by Velte et al. [3] that was developed and applied to show the helical symmetry of the vortices generated by a passive rectangular vane-type vortex generator. Regarding models incorporated into codes,

most are based on the BAY-model by Bender et al. [4] such as the actuator VG model (AcVG) developed in [5], which introduces body forces using source terms in the momentum and/or energy equations to simulate the presence of a vane.

VGs are usually triangular or rectangular vanes inclined at an angle of attack to the oncoming flow and dimensioned in relation to the local boundary layer thickness to allow for the best interaction between the generated vortex wake and the boundary layer, and are usually placed in groups of two or more upstream of the flow separation area, Anderson [6]. For several flow-control applications, conventional VGs first introduced by Taylor [7, 8, 9] have been successfully applied onto aircraft wings for flow control that enhance mixing of the boundary layer and thus transferring high momentum fluid closer to the wall, thereby suppressing or delaying separation, Schubauer [10]. Furthermore, the experimental work carried out by Velte [11] and the corresponding simulations made by Fernández-Gámiz *et al.* [12] showed that the primary vortex produced by a rectangular VG mounted on a flat plate achieves self-similarity for both axial and azimuthal velocities. In most applications, VGs are designed with the device height h on the order of the local boundary layer thickness δ and are mounted normal to the surface with an angle of incidence to the oncoming flow to generate streamwise longitudinal vortices. Nevertheless, in some flow-control application, the residual drag associated to these relatively large δ-scale VGs could be excessive.

A practical and fairly simple method to improve the VG efficiency is by generating the streamwise vortices using vanes with reduced device height. Lin *et al.* [13] demonstrated that by reducing the height of the conventional VGs to a fraction of the local boundary layer, the devices still provide enough momentum transfer downstream of the VG, especially in turbulent boundary layers where the velocity profile is relatively full. These low-profile (sub-δ-scale) VGs were successfully implemented on multi-element high-lift airfoils to control flow separation on the flap. Yao *et al.* [14] made a comparison of the effects on the vortex trajectory between a low-profile VG with the device height approximately equal to 20 percent of the boundary layer thickness and a conventional VG with $h = \delta$. Furthermore, the experimental and theoretical study carried out by Ashill et al. [15] revealed a successful delaying of the shock-induced separation on a transonic airfoil by the implementation of Sub Boundary Layer Vortex Generators (SBVG). It was found that wedge SBVGs give significant increases in lift and reductions in drag. According to Lin [16], the low-profile VGs are one of the best options when the flow-separation locations are relatively fixed and the devices can be mounted reasonably close upstream of the separation.

The success of implementing low-profile VGs to achieve performance improvements in several aerodynamic applications led to an increased focus on providing detailed information in the wake downstream of these devices for a better understanding of the physics of the flow.

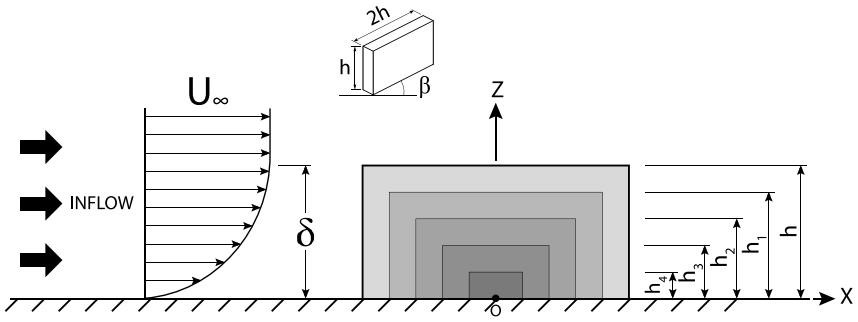

Figure 1. VG dimensions.

The main objective of this work is to study the variation of the path of the primary vortex generated by a rectangular VG mounted on a flat plate with five different device heights $h = \delta$, $h_1 = 0.8\delta$, $h_2 = 0.6\delta$, $h_3 = 0.4\delta$ and $h_4 = 0.2\delta$, where δ is the local boundary layer thickness and h_i represents the height of the low-profile VGs for each case, as sketched in figure 1. For this purpose, computational simulations have been carried out using RANS method and at Reynolds number $Re = 1350$ based on the boundary layer thickness at the VG position of $\delta = 0.25m$. The case consists of a single vortex generator on a flat plate with the angle of attack of the vane to the oncoming flow $\beta = 18.5°$. The flow over the flat plate without the VG has been previously simulated to calculate the boundary layer thickness at the VG position.

This study of the vortex development of low-profile VGs can contribute to obtain a better understanding of the behaviour of the wake downstream of these types of vortex generating devices and, therefore, to take advantage of the benefits of these vanes, such as their intrinsic simplicity, cheap implementation and low drag.

2. Computational configuration

In this study, steady state simulations were carried out and performed with a structured finite-volume flow solver using, in this work, Reynolds-Averaged Navier-Stokes equations. The convective terms are discretized using the third order Quadratic Upstream Interpolation for Convective Kinematics (QUICK scheme), [17]. For these computations the $k - \omega$ SST (Shear Stress Transport) turbulence model by Menter [18] was used. A successful validation of steady RANS simulations against measurements is the one carried out by Allan [19], where the flow field about a single low-profile VG on a flat plate with two different vane angle-of-attack of 23° and 10° was computed using OVERFLOW, a flow solver code developed at NASA. The results of these simulations were compared to experimental data and showed that the CFD and experiments agreed well except for short distances downstream of the vane.

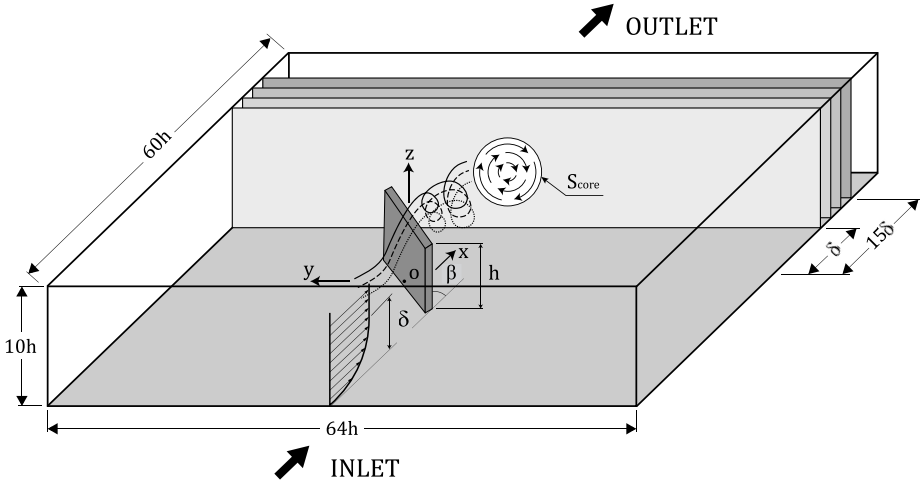

Figure 2. Computational domain (not to scale).

Figure 2 illustrates the computational setup with the current setting consisting of a single VG on a flat plate. The dimensions of the computational domain normalized with the conventional VG height h are also given in figure 2. The thickness of the vane is constant and the VG was positioned normal to the wall at a position where the local boundary layer thickness is equal to the conventional VG height $\delta = h$. The actuator is a rectangular vane with a length twice the VG height for all cases, as sketched in figure 1. Previously, the flow over the flat plate without the VG was simulated to model the evolution of the boundary layer. The VG was placed at

the position where local boundary layer thickness was equal to 0.25m, approximately forty two times the local boundary layer thickness (42δ) downstream of the inlet.

The VG angle of attack to the oncoming flow is β=18.5^o and the Reynolds number based on the VG height h= 0.25m is Re= 1350, using an inflow velocity U_∞= 1ms^{-1} and a density of 1 kgm^{-3}. The vane angle is very close to the optimum found by Godard *et al.* [20] in a parametric study optimizing separation control. The computational setup of the CFD simulations consists of a block structured mesh of 25 million cells with the first cell height $(\Delta z/h)of 1.5\times10^{-5}$ normalized by the height of the conventional VG. In the immediate vicinity of the vane, the mesh has 6.5×10^6 cells, while the mesh downstream of the VG for capturing the wake has approximately 11.5×10^6 cells, see figure 3(a,b). In order to resolve the boundary layer, cell clustering has been used close to the wall and the dimensionless distance from the wall is less than 1 ($y^+ < 1$). Verification of enough mesh resolution was performed by a mesh independency study, where the results obtained from the finest mesh (Grid 1 with 25 million cells) are compared with the results from the medium (Grid 2 with 12 million cells) and the coarsest mesh (Grid 3 with 6.5 million cells).

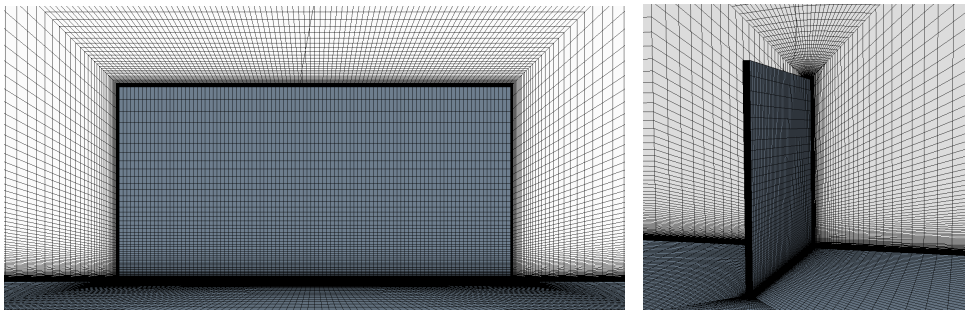

(a) Longitudinal section. (b) Cross-flow section.

Figure 3. Mesh sections on the VG position.

Figure 4 illustrates the axial velocity profiles for all grid levels for the case of the conventional VG h. These profiles were extracted in a plane normal to the flow direction at five local boundary layer thicknesses downstream of the vane and along a line parallel to the wall passing through the center of the primary vortex. A mesh dependency of around $\sim 2\%$ has been detected.

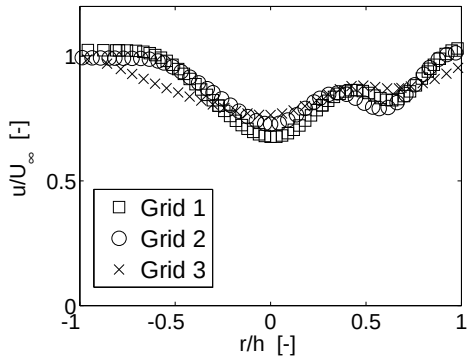

Figure 4. Axial velocity profiles for three different mesh sizes of the computations.

All the velocity components and the vortex center position coordinates were extracted in the simulations in 15 spanwise planes, normal to the wall and located from 1 to 15 boundary layer thicknesses downstream of the vortex generator, as sketched in figure 2.

3. Results

Numerical simulations of the vortex generating vane on a flat plate were performed. Four dimensions of a single low-profile vane $h_1 = 0.8\delta$, $h_2 = 0.6\delta$, $h_3 = 0.4\delta$ and $h_4 = 0.2\delta$ at β=18.5^o were computed and compared with the results of the conventional VG $h = \delta$. The extraction of the data from the computations was conducted in a similar way to the procedure described in [12], in planes normal to the wall downstream of the VG to capture the development of the vortex.

Table 1 shows the height of the conventional VG h and the heights of the low-profile (sub-δ-scaled) VGs with the corresponding Drag coefficients C_D. The heights of the low-profile VGs have been designed with a reduction factor of 20% with respect to the height of the conventional VG. However, this decreasing rate in the VG height is not followed by the Drag coefficients, as presented in the fifth column of the table 1. The Drag coefficient of the smallest VG h_4, with a height of 20% of the conventional VG height, has the 44% of the Drag of the largest VG h. Note here that the increase of the Drag on an aerodynamic body due to the implementation of VGs is not only related to the Drag of the vanes themselves, but also to the change in the body boundary layer features downstream of the vanes position.

Table 1. VG heights and Drag coefficients.

VG	% of δ	Height (m)	C_D	ΔC_D(%)
h	100	0.25	0.1786	100
h_1	80	0.20	0.1585	88
h_2	60	0.15	0.1340	75
h_3	40	0.10	0.1054	59
h_4	20	0.05	0.0796	44

In order to analyze the vortex evolution, up to three parameters were previously identified regarding vortex development from past studies on streamwise vortex embedded in turbulent boundary layers, Bray [21] and Yao *et al.* [14]. Therefore, the vortex generating devices are characterized by the peak streamwise vorticity $\mid \omega_x \mid_{max}$, vortex circulation Γ and location of the vortex core. The peak vorticity is used to locate the center of the streamwise vortex in each plane position downstream of the VG and, subsequently, to determine the vortex path, which is the main objective of this work. According to Pearcy [22] and Ashill *et al.* [15], the circulation is a parameter associated to the vortex induced rate of mixing of the outer flow with the boundary layer. The trajectory of the primary vortex generated by a vane-type VG plays also a determining role in the mixing performance.

By observing the location of the vortex center as a function of the downstream axis x, one can determine the trajectory of the vortex in both lateral (y) and vertical (z) directions. Figures 5 shows a comparison between the trajectories described by the vortex generated by a conventional VG h and the trajectories of the low-profile VG vortices h_1, h_2, h_3 and h_4. Streamwise coordinates are normalized by the local boundary layer thickness δ and both lateral and vertical coordinates are normalized by the corresponding VG height for each VG, represented by h_i, to show the effects of VG scaling downstream of the vane.

The lateral path of the conventional VG h and the lower profile VGs h_1, h_2 and h_3 tend to follow the direction in which the device is pointed, see figure 5(a). However, in the case of the lowest VG h_4, the lateral path stays almost parallel to the flow direction when far from the VG and achieves the smallest deviation in the vortex core in the y direction in comparison with the

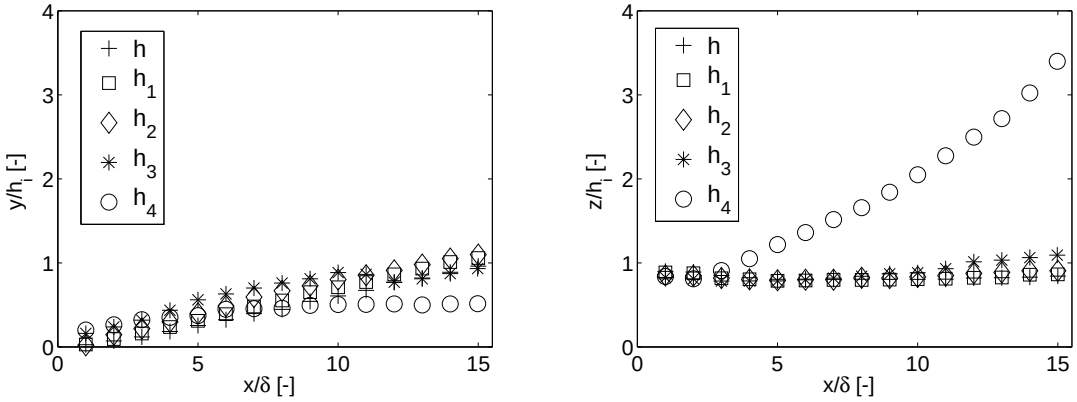

(a) Non-dimensional lateral path. (b) Non-dimensional vertical path.

Figure 5. Influence of VG scaling on vortex core trajectory. Note that both lateral and vertical paths are normalized by the corresponding device height h_i. The streamwise distance x is normalized by the boundary layer thickness at the VG position δ.

other cases. Close to the VG, all the trajectories start from almost the same point independently of the VG height. The largest deviation in the lateral path is reached by the VG h_2, which is 1.1 device heights at the plane position $x/\delta = 15$. Nevertheless, at the positions up to $x/\delta = 10$ the highest variation in the lateral vortex trajectory is reached by the VG h_3.

The vortex paths in the vertical direction are represented in figure 5(b) As in the case of the lateral path, the vertical positions are also normalized by the corresponding VG height. Figure 5(b) shows that the vertical trajectories roughly collapse in the streamwise plane positions studied. This means that, in absolute terms, the vertical trajectory of the VGs decreases proportionally as the VG height decreases and stays roughly within the order of the corresponding device height, except for the case of the lowest profile h_4, which behaves quite differently. In this case the slope of the vertical path is much higher than all other cases, thus at positions far away from the VG the elevation of the vortex center is very large in comparison with the other VGs. Note that the vortex location for every plane position remains within the boundary layer and stays approximately parallel to the wall, except for the case of the smallest vane h_4.

The normalized vortex paths for the low-profile VGs follow the same trends for both lateral and vertical direction of the conventional VG except for the lowest VG h_4. In this case, the slope of the vertical path is much higher than the other cases, above all far away the VG. In 1933 Prandtl argued that for the inner law, the boundary layer profile would depend upon wall stress τ_w, fluid properties (density ρ and dynamic viscosity μ) and vertical distance from the wall z, but not upon freestream parameters: $\bar{u} = fcn(\tau_w, \rho, \mu, z)$. Conversely, Kármán reasoned in 1930 that, for the outer layer, the wall acts merely as a source of retardation, reducing local velocity $\bar{u}(z)$ below the freestream velocity in a manner independent of dynamic viscosity but dependent upon wall shear stress, boundary layer thickness and pressure gradient. Therefore, due to the low height of the vane, the vortex generated by the VG h_4 is very close to the inner part of the boundary layer where the viscous (molecular) shear is prevailing, thus there is strong interaction with the wall. According to White [23], what happens very near the wall is that the turbulence is damped out and the inner boundary layer is dominated by the viscous shear. This could be one of the reasons for the different behavior.

In addition to the above in the lateral and the vertical paths of the vortex, the maximum value of the streamwise vorticity has been studied. To illustrate the vortex decay, the streamwise

distribution of the normalized peak vorticity $(\omega_{x,max}\ h_i)/U_\infty$ is plotted as a function of the non-dimensional downstream distance x/δ for all cases studied. Figure 6(a) shows the decay of the vortex in the streamwise direction and confirms that the peak vorticity is rapidly attenuated downstream of the VG for all cases except for the conventional VG. In this case, the maximum value of the streamwise peak vorticity is reached immediately downstream of the device at the position $x/\delta = 3$. The peak vorticity decays exponentially and inversely proportional to x/δ. As expected, the magnitude of the peak vorticity decreases as the height of the VG is reduced.

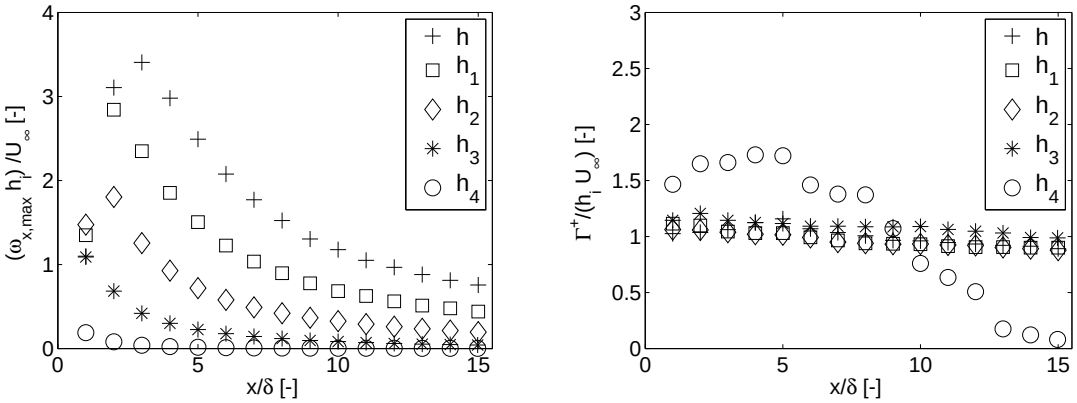

(a) Non-dimensional stream-wise peak vorticity. (b) Non-dimensional positive circulation.

Figure 6. Influence of VG scaling on vortex decay and vortex strength.

The strength of the vortex is evaluated in this work by the positive circulation (Γ^+) defined by the equation (1), which is calculated by finding the vortex center position from the peak vorticity over the area surrounding the vortex core in cross-flow plane positions normal to the wall, as sketched in figure 2, and it has been normalized by the corresponding VG height h_i and by the free-stream velocity U_∞. The resulting streamwise distribution of the normalized positive circulation $\Gamma^+/(h_i\,U_\infty)$ is represented in figure 6(b).

$$\Gamma^+ = \int_S \omega_x^+ dS \tag{1}$$

The non-dimensional positive circulation barely varies at the streamwise stations studied for the VG cases h, h_1, h_2 and h_3. Thus, this means that the non-dimensional positive circulation is independent of the vane height for cases where device heights are located in the outer part of the boundary layer, which is in agreement with Ashill *et al.* [15]. However, once again, the behaviour of the VG h_4 is significantly dissonant with respect to the other VGs. The non-dimensional circulation development of the VG h_4 in the streamwise direction is considerably different from the other low-profile VGs and its maximum value is reached at the streamwise station of $x/\delta = 4$ and then decreases due to viscous dissipation and reaches values close to zero at positions far away from the VG. In general, the decay of the circulation is more linear in comparison with the decay of the peak vorticity. The trends of the circulation decay follow approximately similar trajectories, except for the lowest VG h_4, as has been previously mentioned. Apparently, this occurs because the vortex generated by the lowest VG is very close to the wall and consequently close to the inner part of the boundary layer where the viscous shear is dominant. Viscosity does not control the whole shear layer but only a thin part close to the wall (the so-called near-wall layer) while viscous effects can be safely neglected in the outer layer.

Additionally, two plots have been created to visualize the effect of the vane height scaling on the vortex development at three plane positions downstream of the VG $x/\delta = 5$, $x/\delta = 10$ and

$x/\delta = 15$. Figures 7(a) and 7(b) illustrate the influence of VG scaling on vortex peak vorticity and vortex strength, respectively. In the horizontal axis of these plots the VG height as a percentage of the local boundary layer thickness is represented (as shown in table 1), indicating as well, the corresponding vane notation.

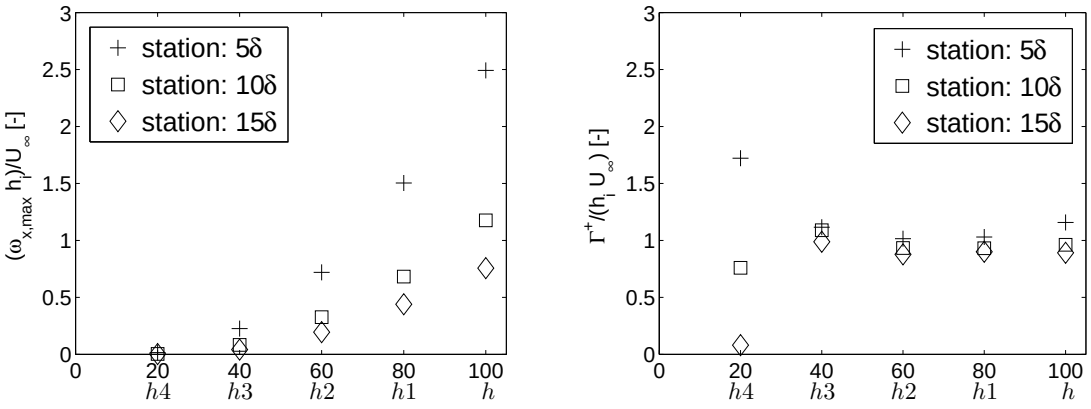

(a) Non-dimensional stream-wise peak vorticity.

(b) Non-dimensional positive circulation.

Figure 7. Influence of VG scaling on vortex development at three plane positions downstream of the VG 5δ, 10δ and 15δ.

For all VG cases, the non-dimensional peak vorticity increases as the device height increases and the maximum values are reached at the streamwise station of $x/\delta = 5$. The conventional VG h has much lager values of normalized peak vorticity in comparison with the lower profile VGs. The smallest values of peak vorticity correspond to the lowest vane h_4. Probably, due to its reduced size it is not able to generate as much vorticity as the other vanes. As shown in figure 7(a), the low-profile VGs h_1, h_2, h_3 and h_4 follow the trend of the conventional VG h and it seems that the evolution of the non-dimensional peak vorticity (normalized by the corresponding VG height) increases exponentially with the device height.

Regarding the vortex strength, figure 7(b) presents the values of the non-dimensional circulation against the device heights at three stations, in the same manner as was previously done with the peak vorticity. It is clear in this plot that normalized circulation remains roughly constant at the three plane stations for all vanes, with the exception of the lowest VG h_4. This shows that the non-dimensional positive circulation reached at these plane positions does not depend on the vane height and the variation of the normalized circulation with the device height can reasonably be ignored for devices that are located in the outer part of the boundary layer. This outcome is strongly in accordance with the results presented in Betterton *et al.* [24]. Once more, it is worth noting the different behavior of the lowest VG h_4, which reaches the largest value of the normalized circulation at the first station 5δ and then decays rapidly until almost zero in the third station 15δ.

Of the five types of VG studied, h, h_1, h_2, h_3 and h_4, the last one was the most effective in terms of producing non-dimensional positive circulation just downstream of the device at the streamwise station of 5δ. The vane h_4 produces similar or even larger normalized circulation up to the station 9δ but, thereafter, decreases rapidly until values close to zero. The non-dimensional positive circulation for the other cases stays almost constant at the three streamwise stations evaluated. This means that the normalized circulation does not depend on the device height in the streamwise distance studied from 5δ to 15δ for the cases h, h_1, h_2 and h_3. However, with a notable difference to the rest, the VG case h_3 has a drag coefficient 41% lower than the conventional one. In terms of VG efficiency (measured as non-dimensional circulation

production) to additional drag, it seems that the device height h_3 could be a more efficient alternative to the conventional VG due to its much lower drag and because it produces a similar level of non-dimensional circulation.

4. Conclusions

Vortices generated by rectangular vane-type vortex generators of the same and lower height than the local boundary layer thickness on a flat plate have been investigated. The ultimate goal of this study is to contribute to obtain a better understanding of the behaviour of the primary vortex downstream of the so-called low-profile vortex generators and, consequently, to make the most of the main advantages of these vanes, such as their intrinsic simplicity, cheap implementation and low drag. Hence, computational simulations of these passive devices within a turbulent boundary layer flow over a flat plate at Reynolds number $Re = 1350$ based on the conventional VG height $h = 0.25$ m and free stream velocity $U_\infty = 1$ ms^{-1} have been carried out using the RANS method.

The VG scaling significantly affects the trajectory and non-dimensional steamwise peak vorticity of the vortex generated by vane-type VGs. The normalized vortex trajectories of the low-profile VGs h_1, h_2 and h_3 follow the general trends of the conventional VG h. However, the path of the vortex h_4 is considerably different for both lateral and vertical direction in comparison with the conventional VG and the other low-profile devices. One reason for this different behaviour could be attributed to the fact that the vortex generated by the vane h_4 is very close to the wall, probably interfering with the inner part of the boundary layer, where the viscous shear stress is dominant and, thus, there is considerable interaction with the wall.

In terms of the ratio effectiveness to additional VG drag, the case h_3 seems to be the most promising VG configuration. In comparison with the case of the conventional VG, h_3 produces the same or even larger amount of normalized circulation downstream of the vane with much lower device drag. The case of h_4 produces the highest non-dimensional circulation at stations close to the trailing edge of the VG, nevertheless, its rapid decay in the streamwise direction makes this configuration less efficient than the case of h_3.

As a future work, it would also be interesting to study in detail how the modified boundary layer downstream the VG affects the total drag of an aerodynamic object (in addition to the parasitic drag of the VG itself) and to carry out more CFD simulations at higher Reynolds numbers. Of course, wind tunnel experiments to validate the present computations are highly desirable.

5. Acknowledgments

This work was supported by both the Government of the Basque Country and the University of the Basque Country UPV/EHU through the SAIOTEK (S-PE11UN112) and EHU12/26 research programs, respectively. Technical and human support provided by IZO-SGI, SGIker (UPV/EHU, MICINN, GV/EJ, ERDF and ESF) is gratefully acknowledged. Computations were made using of ARINA PC-cluster at UPV/EHU. The authors also wish to acknowledge CD-Adapco for providing the CFD solver.

References

[1] Gad-el-Hak M 2007 *Flow Control: Passive, Active, and Reactive Flow Management* 1st ed (Cambridge University Press)
[2] Smith F T 1994 *Journal of Fluid Mechanics* **270** 91–131
[3] Velte C M, Hansen M O L and Okulov V L 2009 *Journal of Fluid Mechanics* **619** 167–177
[4] Bender E E, Anderson B H and Yagle P J 1999 *American Soc.of Mechanical Engineers FEDSM99-6929 New York*

[5] Fernández-Gámiz U, Réthoré P E, Sørensen N N, Velte C M, Zahle F and Egusquiza E 2012 Comparison of four different models of vortex generators (European Wind Energy Conference EWEA)
[6] Anderson B H 29th Aeroespace Sciences Meeting, Nevada, 1991 The aerodynamic characteristics of vortex ingestion for the fla-18 inlet duct
[7] Taylor H D 1947 The elimination of diffuser separation by vortex generators Research department report no. r-4012-3 United Aircraft Corporation, East Hartford, Connecticut
[8] Taylor H D 1948 Application of vortex generator mixing principles to diffusers Research department concluding report no. r-15064-5 United Aircraft Corporation, East Hartford, Connecticut
[9] Taylor H D 1950 Summary report on vortex generators Research department report no. r-05280-9 United Aircraft Corporation, East Hartford, Connecticut
[10] Schubauer G B and Spangenber W G 1960 *Journal of Fluid Mechanics* **8** 10–32
[11] Velte C M 2012 *AIAA Journal (ISSN: 0001-1452)* **51** 526–529
[12] Fernández-Gámiz U, Velte C M, Réthoré P E and Sørensen N N 2012 Self-similarity and helical symmetry in vortex generator flow simulations (Torque 2012, The science of making torque from wind, Oldenburg)
[13] Lin J C, Howard F G and Selby G V 1990 *Journal of Spacecraft and Rockets* **27** 503–507
[14] Yao C S, Lin J C and Allan B G 24-27 June 2002 Flow-field measurement of device-induced
[15] Ashill P R, Fulker J L and Hackett K C 8-11 January 2001 Research at DERA on sub boundary layer vortex generators (SBVGs) (39th Aerospace Sciences Meeting and Exhibit, Reno, Nevada)
[16] Lin J C 2002 *Progress in* **38** 389–420
[17] Khosla P K and Rubin S G 1974 *Computer Fluids* 207–209
[18] Menter F R 1993 *AIAA Journal* **93-2906**
[19] Allan B G June 24-27 2002 Numerical simulations of vortex generators and jets on a flat plate 1st AIAA Flow Control Conference (AIAA)
[20] Godard G and Stanislas M 2006 *Aerospace Science and Technology* **10** 181–191 dOI: 10.1016/j.ast.2005.11.007
[21] Bray T B 1998 *A parametric study of vane and air-jet vortex generators* EngD dissertation Cranfield University, UK
[22] Pearcey H 1961 *Shock induced separation and its prevention by design and boundary layer control. In Boundary Layer and Flow Control* (Pergamon Press)
[23] White F M 1991 *Viscous Fluid Flow* 3rd ed (McGraw-Hill, Singapore) pp. 470-481
[24] Betterton J G, Hackett K C, Ashill P R, Wilson M J and Woodcock I J 2000 Laser doppler anemometry investigation on sub boundary layer vortex generators for Tech. rep. DERA Bedford, UK and Air force Research Laboratory, USA